Science of Sintering, **54** (2022) 189-200

https://doi.org/10.2298/SOS2202189S

UDK: 692.533.1; 666.3-127; 53.086

Preparation and Characterization of Novel Glycidyl Methacrylate/Clay Nanocomposites

Ivan S. Stefanović[1*)], Bojana M. Marković[1], Aleksandra B. Nastasović[1], Zorica M. Vuković[1], Aleksandra Dapčević[2], Vladimir B. Pavlović[3]

[1]Institute of Chemistry, Technology and Metallurgy, National Institute (ICTM), University of Belgrade, Njegoševa 12, 11000 Belgrade, Serbia

[2]Faculty of Technology and Metallurgy, University of Belgrade, Karnegijeva 4, 11000 Belgrade, Serbia

[3]Faculty of Agriculture, University of Belgrade, Nemanjina 6, 11000 Belgrade, Serbia

Abstract:

The impact of the type and amounts of nanofiller on the features of the glycidyl methacrylate-co-ethylene glycol dimethacrylate (GMA-co-EGDMA)/organomodified montmorillonite (OMt) nanocomposites that were prepared by in situ radical suspension polymerization, was examined. Cloisite 30B and Cloisite 25A were used in this study as nanofillers, in amounts of 2 and 10 wt.%. The structure, morphology, thermal stability and porosity of the initial GMA-co-EGDMA copolymer and their nanocomposites were examined by ATR-FTIR analysis, wide angle X-ray diffraction (XRD), scanning electron microscopy with energy-dispersive X-ray spectroscopy (SEM-EDS), transmission electron microscopy (TEM), thermogravimetric analysis (TG) and mercury porosimetry. It has been established that both clay nanofillers were successfully incorporated into the structure of the initial copolymer, simultaneously on their surface and also on cross-sectional area. Prepared samples with 2 wt.% have predominantly exfoliated, while samples with 10 wt.% have some tactoids-aggregates structure of the OMt layers. Thermogravimetric analysis revealed that after ~ 30 % of degradation, all nanocomposites become more thermal stable than the initial copolymer. The obtained results indicate that porosity parameters can be easily modified with the addition of clay nanofillers and thus prepared nanocomposites adjusted to specific purposes.

Keywords*: GMA-co-EGDMA Nanocomposites; Clay nanofillers; Morphology; Thermal properties; Porous structure.*

1. Introduction

Macroporous copolymer beads, based on glycidyl methacrylate (GMA) and ethylene glycol dimethacrylate (EGDMA), attract a lot of interest and have been extensively used in recent years for different purposes. GMA represents an important vinyl monomer which can be used to obtain high chemical stability, high tensile strength, non-toxicity and hydrophilic nature of the final polymers [1,2]. In addition, GMA-*co*-EGDMA copolymers are often obtained in the form of macroporous beads, with very attractive porosity that can be easily adapted and optimized by adjusting the composition and conditions of the reaction mixture. Also, it offers a large surface area, with a plenty of high reactive epoxy groups in the side of

*) **Corresponding author:** ivan.stefanovic@ihtm.bg.ac.rs

their polymer chains, suitable to do various chemical functionalization for heavy metal ion and textile dyes removal [3,4], protein separation [5] and supports for controlled release of enzymes [6], drugs [7] or antibacterial agents [8].

Despite all these good features, GMA-*co*-EGDMA still needs to enhance some chemical and physical performances. One of the possible ways to do this is to incorporate different nanoparticle fillers (at very low weight content), such as layered silicates i.e. clays, inside the polymer structure. The aim is to obtain well dispersed single clay sheets inside the polymer structure, in order to achieve improvement of the barrier, thermal, mechanical, surface, electrical and flame retardancy properties [9-12]. However, the preparation of the clay-polymer nanocomposites is quite demanding, due to the fact that natural silicates, such as montmorillonite (Mt), are hydrophilic while on the other side polymer matrix is organophilic in nature. The incompatibility between them can be overcome by use previously organically modified clays (for example with alkylammonium or alkylphosphonium ions). In this way, the replacement of alkali cations by these ions, allows obtaining good and homogenous dispersion and improved interfacial interactions between nanofillers and polymer structure [13-15]. These polymer/clay nanocomposites can be prepared by *in situ* intercalative polymerization, solution intercalation, polymer melt intercalation method, etc [9,16,17]. In these ways, the distance between the clay layers should be increased in order to achieve a complete delaminated structure (exfoliated), or partially separated - some stacked clay structure (intercalated), or undesirable microcomposite structure (unintercalated) in the polymer matrix [18,19].

Çelik et al. [2] prepared several poly(GMA) nanocomposites by free-radical polymerization using Mt clay, that has not been modified previously in any way. Still, they have shown that in this way it is possible to obtain nanocomposites with good clay layers dispersion and also with better thermal stability than pure poly (GMA). In relation to this, Someya et al. [9] prepared novel poly(glycidyl methacrylate-*co*-methyl methacrylate) nanocomposites by introducing various OMt clay, in an amount of 3 and 5 wt.%. They have shown that the highly intercalated nanocomposites were obtained with a clay content of 3 wt.% and that with further increasing of its content up to 5 wt.%, the degree of intercalation was significantly decreased. Salmi-Mani et al. [13] prepared GMA nanocomposites by *in situ* living free-radical photopolymerization previously modifying clay with diazonium salt. They have shown that this was a very effective way to obtain intercalated nanocomposites, since such modified clay can serve not only for nano-reinforcements of GMA, but also as an excellent macro-photoinitiator for polymerization of GMA.

The aim of this paper is to obtain GMA-*co*-EGDMA nanocomposites using two different organomodified montmorillonite clays, in an amount of 2 and 10 wt.%, by *in situ* radical suspension polymerization. The influence of the type and content of organoclays on the structure, porosity, thermal properties as well as morphology of such prepared nanocomposites was examined by different experimental techniques, in order to obtain improved features than neat GMA-*co*-EGDMA copolymer.

2. Experimental Procedures

2.1. Materials

Glycidyl methacrylate (GMA, purity 97 %) and ethylene glycol dimethacrylate (EGDMA, purity ≥98%) were purchased from Merck and Sigma-Aldrich, respectively. Cloisite 30B and Cloisite 25A are commercial organically modified natural Mt clays, modified with methyl-tallow-*bis*-2-hydroxyethyl and dimethyl-2-ethylhexyl hydrogenated tallow quaternary ammonium salt, respectively, where tallow and hydrogenated tallow represent and alkyl group of ~65 % $C_{18}H_{37}$, ~30% $C_{16}H_{33}$ and ~5 % $C_{14}H_{29}$. Clays were purchased from Rockwood, and dried in vacuum oven at 30^{o}C for 24 h, before use. 2,2′-

Azobis(isobutyronitrile) (AIBN) was supplied by Sigma-Aldrich and was purified by recrystallization in methanol. The inert component was consisted of cyclohexanol (purity 98 %, Sigma-Aldrich) and tetradecanol (purity ≥98 %, Merck). Poly(*N*-vinylpyrrolidone) (PVP, Kollidone 90, purity 99 %, BASF) was used as stabilizer. Ethanol (purity 99.8 %) was used for removing the inert components after synthesis and was supplied by Zorka Pharma.

2.2. Preparation of the initial copolymer and their clay nanocomposites

For preparation of nanocomposites the same procedure and reaction conditions were used as in the preparation of the initial copolymer [20]. The only difference is that clay nanofillers were added and sonicated within monomer phase, in the ultrasonic water bath (Fig. 1). Sonication process was used for better incorporation of monomer phase inside the clay interlayer space. The clays were added in quantities of 2 and 10 wt.% relative to the total weight of the monomer phase. The samples were labeled as SGE60-2C30B, SGE60-10C30B, SGE60-2C25A and SGE60-10C25A (SGE means suspension radical copolymerization between GMA and EGDMA, first numbers represent the weight contet of the monomer GMA in samples (60 wt.%), folowed by the number of the weight percent (2 or 10 wt.%) and type of the clay). SGE60 sample represents initial copolymer based on GMA (60 wt.%) and EGDMA (40 wt.%), without clays. The preparation procedure of the initial copolymer and their nanocomposites are shown in Fig. 1.

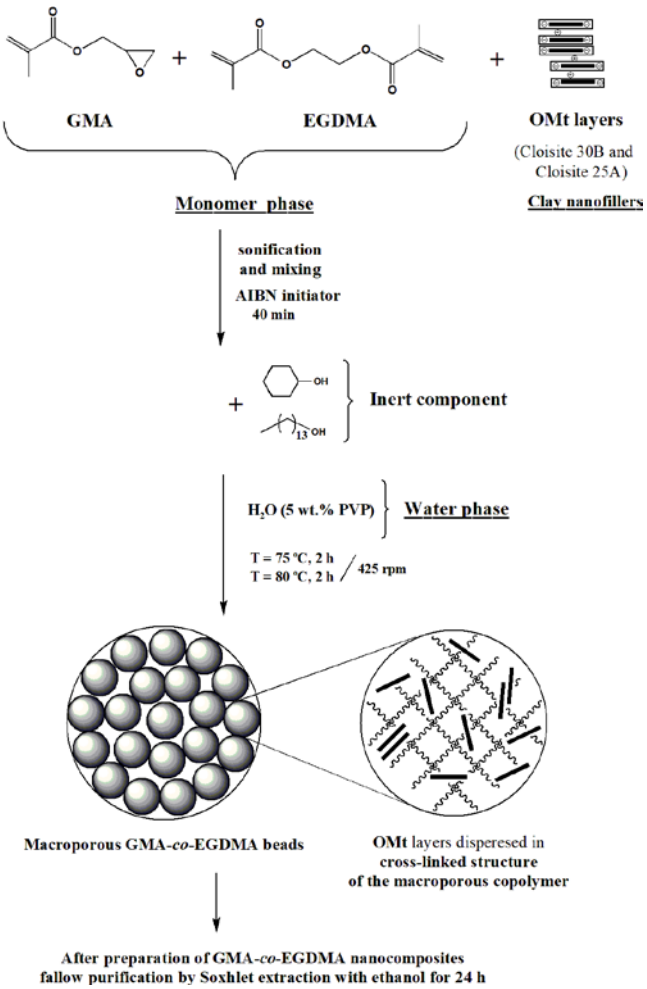

Fig. 1. The scheme of the preparation of the GMA-*co*-EGDMA/clay nanocomposites.

2.3. Characterization methods

FTIR spectra were recorded using ATR mode on a Nicolet 6700 FTIR spectrometer. The scanning range was from 400 to 4000 cm^{-1} at the resolution of 2 cm^{-1} and 64 scans. SEM micrographs were obtained on JEOL JSM-6460LV instrument, at a working distance of *ca.* 14 mm and an accelerating voltage of 20 kV. The samples were coated with a thin layer of Au in high-vacuum evaporator. SEM-EDS analysis was also performed on this instrument that was equipped with X-Max Large Area Analytical Silicon Drift connected with INCA Energy 350 Microanalysis System. XRD analysis was performed on Bruker D8 Advance diffractometer in θ/θ mode, equipped with focusing Ge-crystal primary monochromator, with Cu$K\alpha_1$ radiation (λ=0.15418 nm) (the step-time and step-width for all measurements were 12 s and 0.05°, respectively), in the angle range from 2 to 60°. The nanocomposite beads were cast in Araldite epoxy resin at 60 °C (Fluka) and mounted on holey-carbon coated grids. TEM analysis were perfomed on the JEM-1400 Plus Electron microscope, with a voltage of 120 kV and LaB6 filament, at magnifications of 60k×. Thermal gravimetric analysis was carried out using TGA SDT Q600 V7.0 Build 84 TA instrument, under N_2 atmosphere (the flow rate was 100 mL/min), in the temperature range from 25 to 700°C and at a heating rate of 20 °C/min. The pore size distributions of samples were determined by a high-pressure mercury intrusion porosimeter (Carlo Erba Porosimeter 2000), operating in the interval 0.1–200 MPa and enabling an estimation of the pores in the interval 7.5–15000 nm.

3. Results and Discussion

Among different types of nanoclays, Cloisite 30B and Cloisite 25A were selected for the preparation of these GMA-*co*-EGDMA nanocomposites, due to the fact that these OMt clays show good compatibility and miscibility with epoxy resins. These OMt clays in their structure possess hydroxyl groups that enable hydrogen bonding with carbonyl groups within polymer chains structure [21].

3.1. FTIR analysis

The ATR-FTIR spectroscopy was used to determine the structure of initial SGE60 copolymer, prepared nanocomposites and OMt clays and their ATR-FTIR spectra (from 400 to 1900 cm^{-1} and from 2500 to 4000 cm^{-1}) are shown in Fig. 2.

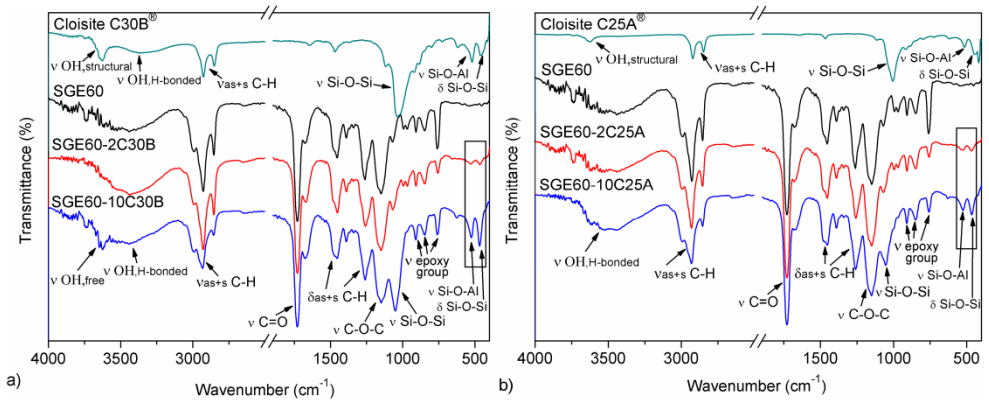

Fig. 2. ATR-FTIR spectra of a) clay Cloisite 30B, initial SGE60 copolymer and obtained nanocomposites with addition of 2 and 10 wt.% Cloisite 30B; and b) clay Cloisite 25A, initial SGE60 copolymer and obtained nanocomposites with addition of 2 and 10 wt.% Cloisite 25A.

In the FTIR spectrum (Fig. 2a) of the Cloisite 30B clay, the folowing bands are observed: 3630 cm^{-1} (ν $OH_{structural}$), 3360 cm^{-1} (ν $OH_{H\text{-}bonded}$), 2935 i 2860 cm^{-1} (ν_{as} and ν_s C-H), 1460 cm^{-1} (δ_{as} C-H and δ O-H), 1040 cm^{-1} (ν Si-O-Si), 520 cm^{-1} (ν Si-O-Al) and at 460 cm^{-1} (δ Si-O-Si). In the FTIR spectrum (Fig. 2b) of the Cloisite 25A clay the same bands at similar values of wavenumbers are observed.

In the FTIR spectrum of the initial SGE60 copolymer, the folowing bands are observed: 3350 cm^{-1} (ν $OH_{H\text{-}bonded}$), 2930 and 2855 cm^{-1} (ν_{as} and ν_s C-H), 1730 cm^{-1} (ν C=O), 1455 and 1260 cm^{-1} (δ_{as} C-H and δ_s C-H), 1150 cm^{-1} (ν C-O-C), and at 760, 850 i 910 cm^{-1} the bands of the epoxy ring vibrations. In the FTIR spectra of all four prepared nanocomposites the bands belonging to SGE60 copolymer are observed, as well as bands at 1050, 525 and 465 cm^{-1} that originate from ν Si-O-Si, ν Si-O-Al and δ Si-O-Si groups, respectively [22,23]. The fact that the bands of both types of clay appeared and that the intensity of these bands is in accordance with the amount of added clays, points out that both clays were well incorporated into the structure of the initial copolymer and that nanocomposites were successfully prepared.

3.2. SEM analysis

SEM microphotographs of the beads surfaces and cross-sections (at magnifications of 5k× and 10k×, respectively) of the initial copolymer and its nanocomposites are shown in Fig. 3.

The surface of the initial copolymer (Fig. 3a) has porous structure, while nanocomposites (Fig. 3b-e) show lower porosity, with more closed pores, as a result of the addition of clay nanofillers. Furthermore, especially in the nanocomposites with 10 wt.% of clays, smaller clay layers-tiles are visible on the surface [24].

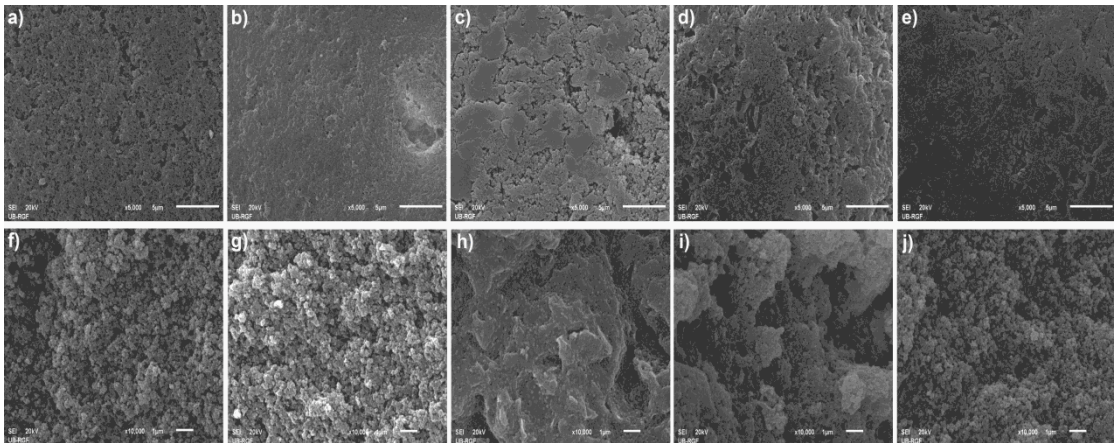

Fig. 3. SEM microphotographs of the beads surface: (a) SGE60, (b) SGE60-2C30B, (c) SGE60-10C30B, (d) SGE60-2C25A, (e) SGE60-10C25A (magnification 5k×); beads cross-section: (f) SGE60, (g) SGE60-2C30B, (h) SGE60-10C30B, (i) SGE60-2C25A and (j) SGE60-10C25A (magnification 10k×).

On the SEM microphotograph of the cross-sectional area of the initial copolymer (Fig. 3f), pronounced three-dimensional porous structure is observed. The porosity of this sample is reflected in the presence of a large number of agglomerates of tiny copolymer globules, divided by channels and pores that together form the basis of macroporous structure. On the other side, the cross-sectional morphology of the prepared nanocomposites is permeated with clay layers, which is especially noticeable in samples with 10 wt.% of clay nanofillers (Fig. 3h and 3j).

Tab. I Results of SEM-EDS analysis of the surface and cross-section area of nanocomposites with 2 and 10 wt.% of Cloisite 30B and Cloisite 25A clays.

Element	Sample			
	SGE60-2C30B	SGE60-10C30B	SGE60-2C25A	SGE60-10C25A
	Surface (wt.%)			
C-K	65.90	62.46	64.24	65.52
O-K	33.64	35.68	35.11	30.71
Al-K	0.25	0.60	0.24	1.21
Si-K	0.21	1.26	0.41	2.56
	Cross-section (wt.%)			
C-K	71.97	68.84	65.66	64.60
O-K	27.53	30.26	33.68	32.97
Al-K	0.27	0.32	0.23	0.81
Si-K	0.23	0.58	0.43	1.62

The elemental composition of the surfaces and cross-sections of the nanocomposites was determined by SEM-EDS analysis, and obtained results are presented in Table I. The SEM-EDS analysis confirmed the presence of all expected elements (C, O, Si and Al). Elements were detected both on the surface and on their cross-sectional area. It is clear that a significantly lower percentage of Si and Al atoms (originate from clays) was detected in samples with 2 wt.% comparing to samples with 10 wt.%. Furthermore, it was observed that the content of the Si and Al atoms was higher on the surface than at the cross-section area, for nanocomposites with 10 wt.% of both types of clay. On the other side, the nanocomposites with 2 wt.% of both types of clay have equal content of the Si and Al atoms regardless scanning area. According to SEM-EDS analysis, the clay nanofillers are not just located on the surface but also inside of the prepared nanocomposites.

3.3. XRD analysis

The obtained XRD patterns of both clays and prepared nanocomposites are presented in Fig. 4. According to literature poly(GMA) displays three wide humps in the region between 10-25, 25-35 and 35-50° 2θ, which indicates the amorphous structure of polymer [25]. Similarly, the obtained nanocomposites based on GMA-*co*-EGDMA (Fig. 4), show wide undefined peaks.

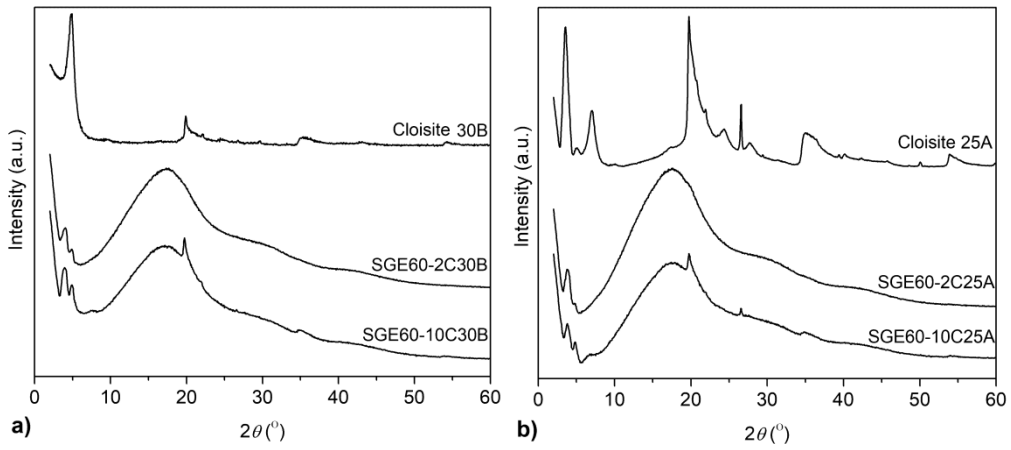

Fig. 4. XRD patterns of the a) Cloisite 30B and their nanocomposites and b) Cloisite 25A and their nanocomposites.

Besides, the main reflections of Cloisite 30B and 25A (at about 5 and 20° 2θ for Cloisite 30B which corresponds to interplanar distances of about 17.7 and 4.4 Å, respectively; and at about 3, 20 and 27° 2θ for Cloisite 25A which corresponds to interplanar distances of about 29.4, 4.4 and 3.3 Å, respectively) are visible in both samples with 10 wt.% of clays indicating the existence of tactoids and undisturbed crystal structures of clay layers. On the contrary, in nanocomposites with 2 wt.% of clays, the sharp peaks above 10° 2θ are absent, but under 10° 2θ are still present, designating that crystalline parts of clays can be separated into an individual layer giving exfoliated or intercalated morphology, but also that some of their parts still remained as tactoids because clays main reflections can be overlapped with the main reflections from initial SGE60 sample [26]. A better explanation and insight into the clay morphology in these samples will give us TEM analysis that is presented below.

3.4. TEM analysis

TEM analysis was also performed in order to determine the clay layers structure and assessment of their dispersion in the prepared nanocomposites. Barring in mind that brighter and transparent regions should represent the neat copolymer matrix (consisted of lighter C, H and O atoms), while the dark lines appeared from individual clay layers (consisted of heavier Al and Si atoms) [27], TEM micrographs of the samples with 2 and 10 wt.% of both clays (Fig. 5) are commented.

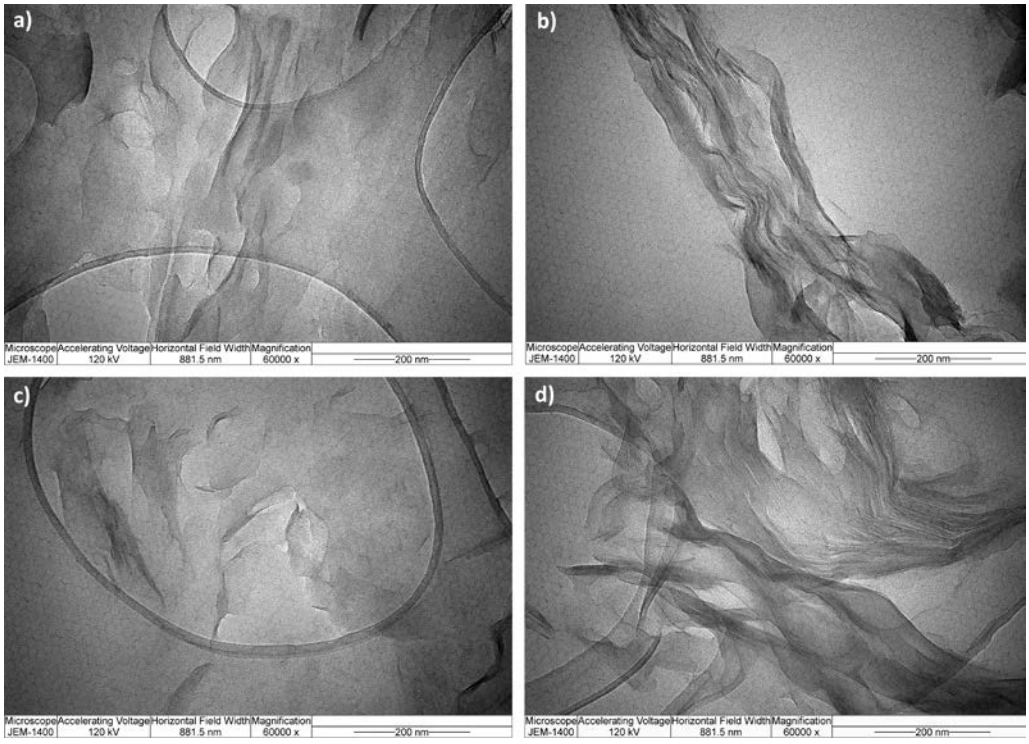

Fig. 5. TEM micrographs of prepared nanocomposites: a) SGE60-2C30B b) SGE60-10C30B, c) SGE60-2C25A, d) SGE60-10C25A (magnification 60k×).

The clay layers within nanocomposites with 2 wt.% of both clays (Fig. 5a and Fig. 5c) were randomly staggered, with morphology that is generally exfoliated and well and homogeneous dispersed in the polymer structure. On the other side, in samples with higher clay content (10 wt.%) (Fig. 5b and Fig. 5d), intercalated morphology is visible besides lousy dispersed tactoids-aggregates of clay layers. The appearance of tactoids-aggregates indicates

that van der Waals forces as well as high specific surface energy still tending to keep them stuck tightly in the polymer structure [27]. These findings are completely in accordance with XRD ones.

3.5. TG analysis

The obtained TG and DTG curves are shown in Fig. 6, while characteristic degradation temperatures and temperatures of DTG peaks are presented in Table II.

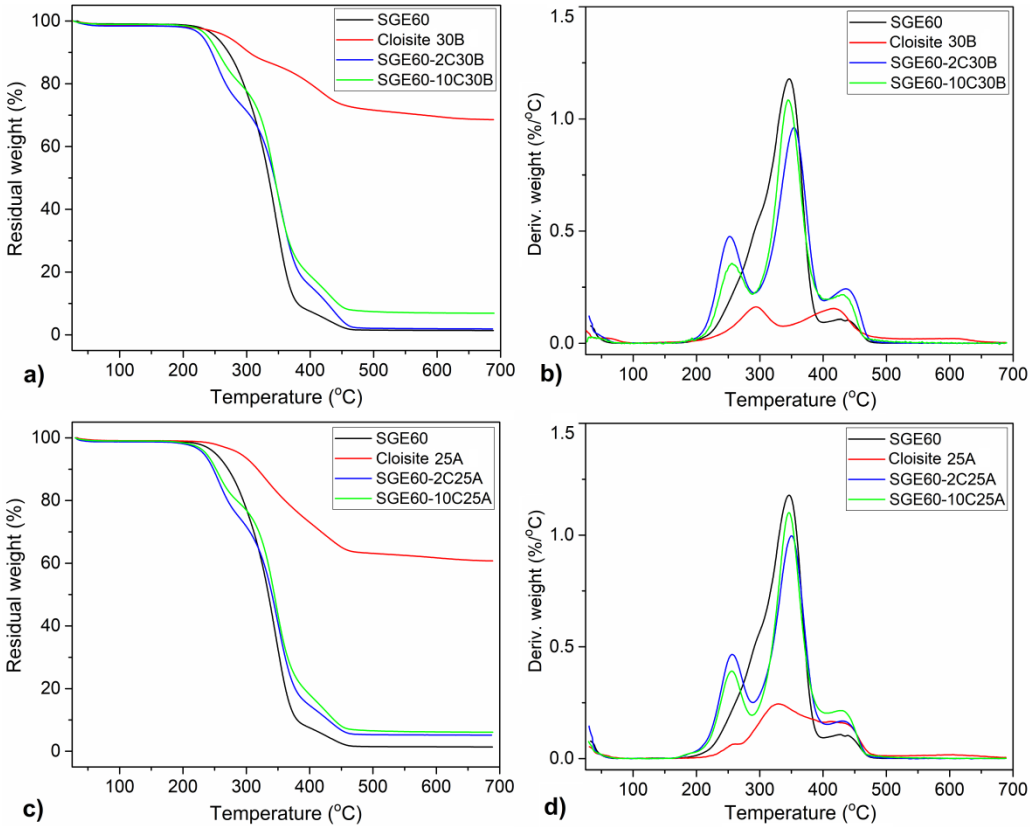

Fig. 6. TG (a) and c)) and DTG (b) and d)) curves of the Cloisite 30B and Cloisite 25A, initial copolymer and their nanocomposites.

Cloisite 30B and Cloisite 25A start to decompose after 304 and 318°C, respectively, and their degradation process took place through three and four steps [28,29]. In both clays, degradation steps are related to the decomposition of organomodifier inside their inorganic structure, while their residual weights at 700°C are quite high and amount of 68.5 and 61.1 % (Table II). The decomposition temperatures that correspond to the mass losses of 10, 50 and 90 % ($T_{10\%}$, $T_{50\%}$ and $T_{90\%}$) of the initial SGE60 copolymer are found at 271, 335 and 380°C. $T_{10\%}$ values for all prepared nanocomposites are lower than for the initial SGE60 copolymer. However, the further thermal degradation shows that after ~ 30 %, all nanocomposites become more thermal stable than the initial SGE60 copolymer. Accordingly, $T_{50\%}$ and $T_{90\%}$ values for all nanocomposites are higher than those for the initial SGE60 copolymer. Moreover, as expected, the nanocomposites with 10 wt.% of both clays are more thermal stable than corresponding nanocomposites with 2 wt.% of clays (Table II), regarding the fact that the clay layers served as a thermal barrier for delaying the elimination of the volatile

compounds and slow down the heat transfer inside the polymer structure, resulting in increased thermal stability of prepared nanocomposites [12].

Tab. II TG results of the Cloisite 30B, Cloisite 25A, initial copolymer and prepared nanocomposites.

Sample	$T_{10\%}$ (^oC)	$T_{50\%}$ (^oC)	$T_{90\%}$ (^oC)	DTG_{max} (^oC)	Residual weight at 700 ^oC (%)
Cloisite 30B	304	-	-	294/418/597	68.5
Cloisite 25A	318	-	-	258/328/424/603	61.1
SGE60	271	335	380	293/346/427	1.4
SGE60-2C30B	245	343	427	253/353/435	1.9
SGE60-10C30B	255	345	444	256/346/431	6.9
SGE60-2C25A	248	340	429	256/350/431	5.2
SGE60-10C25A	252	344	439	255/348/429	6.1

According to the DTG curves, all samples display three degradation steps. The first one between 250-290^{o}C can be associated to the decomposition of pendant epoxy groups. The second one around 350^{o}C is consequence of chain scissions, resulting in the breakdown of copolymer structure into smaller fragments. The third step could be attributed to the total degradation of copolymer and nanocomposites (around 430^{o}C) [20,30]. The residual weight for the initial copolymer is 1.4 %, while for the nanocomposites is higher and it was increased with increasing the clay content into the nanocomposites. According to this, it was evident that inorganic part of clays significantly participates in the creation of char after thermal degradation of these nanocomposites.

3.6. Porosity

The obtained porosity parameters of the initial copolymer and their nanocomposites are shown in Table III, while their cumulative pore volume distribution curves are shown in Fig. 7.

Tab. III The porosity parameters (specific surface area, S_{Hg}, specific pore volume, V_p, pore diameter that corresponds to half of the pore volume, $d_{V/2}$, and total porosity, P) of the initial SGE60 copolymer and their nanocomposites with Cloisite 30B and Cloisite 25A clays.

Sample	S_{Hg} (m^2/g)	V_p (cm^3/g)	$d_{V/2}$ (nm)	P (%)
SGE60	68	0,88	75	49
SGE60-2C30B	75	0,91	84	49
SGE60-10C30B	80	1,12	96	56
SGE60-2C25A	84	1,01	81	51
SGE60-10C25A	89	1,72	170	38

By comparison of the obtained porosity parameters for the initial copolymer and their nanocomposites it can be concluded that porosity properties were significantly changed with the incorporation of these clay nanofillers. According to the obtained values in Table III, it was concluded that with the addition of clay nanoparticles there was an increase in all

porosity parameters (with the exception of *P* values of SGE60-10C25A sample). In that sense, the addition of a larger amount of clay nanofillers (10 wt.%) also led to a further increase of porosity parameters, especially specific surface area, S_{Hg}, and specific pore volume, V_p, values. As can be seen from the obtained cumulative pore size distribution curves is that all samples have an inverse S shape and generally macroporous structure ($d_{V/2}$ > 50 nm, Table III), but still with a great impact on creation of smaller mesopores ($d_{V/2}$ < 50 nm). These obtained results indicate that porosity parameters of initial copolymer can be easily modified in this way and adjusted to specific purposes [31].

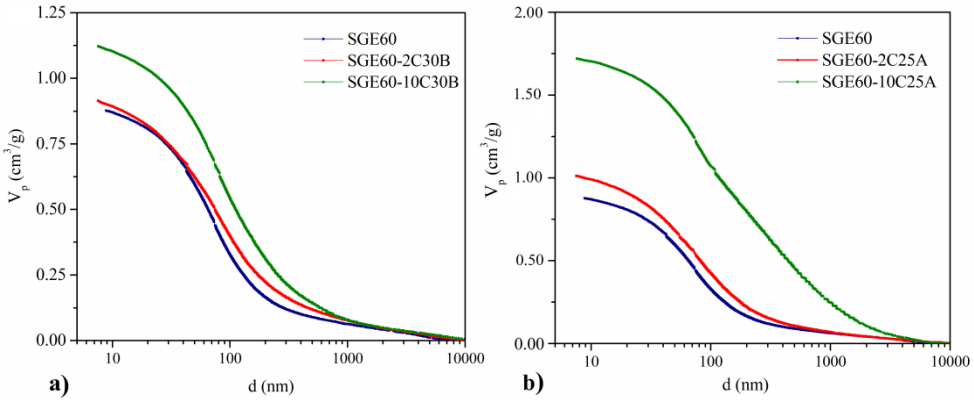

Fig. 7. Cumulative pore size distribution curves for the initial copolymer and their nanocomposites with a) Cloisite 30B and b) Cloisite 25A clays.

4. Conclusion

Novel glycidyl methacrylate-*co*-ethylene glycol dimethacrylate/organomodified montmorillonite nanocomposites that contain 2 and 10 wt.% of clay nanofillers, was successfully prepared by *in situ* radical suspension polymerization. It has been established that both clay nanofillers were incorporated into the structure of the initial copolymer, simultaneously on their surface and on cross-sectional area. Prepared nanocomposites with 2 wt.% have predominantly exfoliated and partly intercalated morphology, while nanocomposites with 10 wt.% possess tactoids-aggregates microstructure of the montmorillonite layers inside the polymer matrix. Thermogravimetric analysis revealed that all samples have good thermal stability and that after ~ 30 % of degradation, all nanocomposites become more thermal stable than the initial copolymer. The obtained results indicate that porosity parameters can be easily modified with the addition of clay nanofillers opening the possibility to adjust nanocomposites to specific purposes. This investigation shows that both clays are a good choice for the preparation of these nanocomposites, emphasizing that Cloisite 25A clay ensures higher values of all porosity parameters of prepared nanocomposites with regard to Cloisite C30B clay. These new glycidyl methacrylate-*co*-ethylene glycol dimethacrylate/montmorillonite nanocomposites can be used as carriers for various immobilizations of enzymes, for sorption of heavy metals and hazardous compounds, or as column material in gas chromatography.

Acknowledgments

This work was financially supported by the Ministry of Education, Science and Technological Development of the Republic of Serbia (Grant No. 451-03-9/2021-14/200026).

5. References

1. X. Wu, W. Jiang, Y. Luo, J. Li, J. Appl. Polym. Sci., 136 (2019) 47441.
2. M. Çelik, M. Önal, J. Appl. Polym. Sci., 94 (2004) 1532-1538.
3. S. Huš, M. Kolar, P. Krajnc, J. Chromatogr. A, 1437 (2016) 168-175.
4. G. Bayramoglu, A. Akbulut, G. Liman, M. Y. Arica, Chem. Eng. Res. Des., 124 (2017) 85-97.
5. N. Dai, S. Wang, H. Li, L. Zhao, H. Jin, N. An, P. Gong, Q. Tan, X. Tang, F. Wang, R. Zhang, J. Chromatogr. B, 1128 (2019) 121794.
6. T. Doğan, E. Bayram, L. Uzun, S. Şenel, A. Denizli, J. Appl. Polym. Sci., 132 (2015) 41981.
7. Y. Wei, Y. Wang, H. Zhang, W. Zhou, G. Ma, J. Colloid Interface Sci., 478 (2016) 46-53.
8. I. D. Vukoje, E. S. Džunuzović, S. Dimitrijević, S. P. Ahrenkiel, J. M. Nedeljković, Polym. Compos., 40 (2019) 2901-2907.
9. Y. Someya, M. Shibata, Polymer, 46 (2005) 4891-4898.
10. S. R. Valandro, P. C. Lombardo, A. L. Poli, M. A. Horn Jr, M. G. Neumann, C. C. S. Cavalheiro, Mat. Res., 17 (2014) 265-270.
11. P. C. LeBaron, Z. Wang, T. J. Pinnavaia, Appl. Clay Sci., 15 (1999) 11-29.
12. I. S. Stefanović, M. Špírková, S. Ostojić, P. Stefanov, V. B. Pavlović, M. V. Pergal, Appl. Clay Sci., 149 (2017) 136-146.
13. H. Salmi-Mani, Z. Ait-Touchente, A. Lamouri, B. Carbonnier, J.-F. Caron, K. Benzarti, M. M. Chehimi, RSC Adv., 6 (2016) 88126-88134.
14. F. A. Bottino, G. Di Pasquale, E. Fabbri, A. Orestano, A. Pollicino, Polym. Degrad. Stabil., 94 (2009) 369-374.
15. A. Hazarika, R. R. Devi, T. K. Maji, Polym. Bull., 68 (2012) 1989-2008.
16. M. Alexandre, P. Dubois, Mat. Sci. Eng. R., 28 (2000) 1-63.
17. K. Jlassi, S. Chandran, M. Mičušik, M. Benna-Zayani, Y. Yagci, S. Thomas, M. M. Chehimi, Eur. Polym. J., 72 (2015) 89-101.
18. M. Kotal, A. K. Bhowmick, Prog. Polym. Sci., 51 (2015) 127-187.
19. O. P. Koc, S. B. Acar, T. Uyar, M. A. Tasdelen, Polym. Bull., 75 (2018) 4901-4911.
20. I. S. Stefanović, B. M. Ekmeščić, D. D. Maksin, A. B. Nastasović, Z. P. Miladinović, Z. M. Vuković, D. M. Micić, M. V. Pergal, Ind. Eng. Chem. Res., 54 (2015) 6902-6911.
21. G. J. Withers, Y. Yu, V. N. Khabashesku, L. Cercone, V. G. Hadjiev, J. M. Souza, D. C. Davis, Composites Part B, 72 (2015) 175-182.
22. M. Kokunešoski, M. Stanković, M. Vuković, J. Majstorović, Đ. Šaponjić, S. Ilić, A. Šaponjić, Sci. Sint., 52 (2020) 339-348.
23. I. Ilić, N. Jović-Jovičić, P. Banković, Z. Mojović, D. Lončarević, I. Gržetić, A. Milutinović-Nikolić, Sci. Sint., 51 (2019) 93-100.
24. P. A. M. Aguilar, M. F. Nicolas, M. Kakazey, R. G. Tapia, M. M. C. Cano, R. A. Matus, T. P. Puig, M. E. S. Nava, M. Vlasova, Sci. Sint., 53 (2021) 137-153.
25. M. Imperiyka, A. Ahman, S. A. Hanifah, M. Y. A. Rahman, Int. J. Polym. Sci., 2014 (2014) 638279.
26. Lj. M. Kljajević, Z. Melichova, D. D. Kisić, M. T. Nenadović, B. Ž. Todorović, V. B. Pavlović, S. S. Nenadović, Sci. Sint., 51 (2019) 163-173.
27. X. Hu, Y. Ke, Y. Zhao, S. Lu, Q. Deng, C. Yu, F. Peng, Colloid. Surface. A, 560 (2019) 336-343.
28. J. M. Cervantes-Uc, J. V.Cauich-Rodríguez, H. Vázquez-Torres, L. F. Garfias-Mesías, D. R. Paul, Thermochim. Acta, 457 (2007) 92-102.
29. H.-S. Kim, B. H. Park, J. H. Choi, J.-S. Yoon, J. Appl. Pol. Sci., 107 (2008) 2539-2544.

30. B. M. Marković, V. V. Spasojević, A. Dapčević, Z. M. Vuković, V. B. Pavlović, D. V. Randjelović, A. B. Nastasović, Hem. Ind., 73 (2019) 25-35.
31. E. M. Bernal, M. Vlasova, P. A. M. Aquilar, M. Kakazey, R. G. Tapia, Sci. Sint. 52 (2020) 25-39.

Сажетак: *Утицај врсте и количине нанопуниоца на својства глицидил-метакрила-ко-етилен-гликол диметакрилата (GMA-co-EGDMA)/ органомодификованих монтморилонит (OMt) нанокомпозита, који су припремљени in situ радикалском суспензионом полимеризацијом, су испитани. Комерцијалне глине (Cloisite 30B и Cloisite 25A) су коришћене у овом раду као нанопуниоци, у количинама од 2 и 10 мас.%. Структура, морфологија, термичка стабилност и порозност полазног GMA-co-EGDMA кополимера и његових нанокомпозита испитани су инфрацрвеном спектроскопијом са Фуријеовом трансформацијом, рендгенском дифракцијом, скенирајућом електронском микроскопијом са енергодисперзивном спектрометрijом, трансмисионом електронском микроскопијом, термогравиметријском анализом и живином порозиметријом. Утврђено је да су оба нанопуниоца глине успешно уграђена у структуру полазног кополимера, истовремено на његовој површини као и на површини попречног пресека. Добијени узорци са 2 мас.% имају претежно ексфолирану структуру слојева глине, док узорци са 10 мас.% показују присуство тактоидних-агрегатих слојева глине. Термогравиметријска анализа је показала да након ~ 30% деградације, сви нанокомпозити постају термички стабилнији од полазног кополимера. Добијени резултати указују да се параметри порозности могу лако модификовати додавањем нанопуниоца глине и на тај начин добити нанокомпозити прилагођени специфичним наменама.*

Кључне речи*: GMA-co-EGDMA нанокомпозити, нанопуниоци глине, морфологија, термичка својства, порозна структура.*